Journal of Digital Imaging

Lossy JPEG Compression in Quantitative Angiography: the Role of X-ray Quantum Noise

Johannes Peter Fritsch[1] and Rüdiger Brennecke[2]

In medical imaging, contrary to applications in the consumer market, the use of irreversible or lossy compression is still in its beginnings. This is due to the suspected risk of compromising the diagnostic content. Many studies have been performed, but it was not until 2008 that national activities in different countries resulted in recommendations for the safe use of irreversible image compression in clinical practice. Quantitative coronary angiography (QCA), however, poses a special problem, since here a large variation in published maximum compression factors has strengthened the general concerns about the use of lossy techniques. Up to now, the reason for the variation has not been thoroughly investigated. Reasons for the discrepancies in published compression factors are determined in this study. Since JPEG compression reduces the quantum noise of the X-ray images, the impact of compression is overestimated when interpreting any change in local diameter as an error. By taking into consideration the quantitative effect of quantum noise in QCA, it is shown that the influence of JPEG compression can be neglected for compression factors up to ten at clinically applicable X-ray doses. This limit is comparable to that found by visual analysis for aesthetic image quality. Future studies on image compression effects should take the interaction with quantum noise explicitly into consideration.

KEY WORDS: Image compression, angiography, coronary arteries, irreversible compression, quantitative coronary angiography, JPEG

INTRODUCTION

Irreversible compression facilitates the efficient storage and transmission of digital images. The application of irreversible compression was established early in the consumer market, boosting the development of technology and devices in this area. In medical imaging, however, the suspected risk of compromising the diagnostic content prevented the widespread application of irreversible compression for a long time. More precisely, two applications have to be distinguished: (1) the use of compressed images for routine visual assessment and (2) their use in quantitative evaluation. This study centers on the second application, but with regard to the aspect of image quality for medical applications, both have to be discussed in context.

Since the introduction of the first international standard for irreversible image data compression, JPEG, in 1992,[1] research has been intensified in both fields.[2] In 2000, Erickson concluded in a publication for the Society for Computer Applications in Radiology, "*Increasing evidence suggests that some forms of irreversible compression can be used with no measurable degradation in aesthetic or diagnostic value.*"[3] Six years later, in 2006, it was stated that "*based on scientific studies, irreversible compression is a clinically acceptable option for the compression of medical images,*" concluding, "*the adoption of irreversible compression as a standard of practice is no longer a matter of 'if' but a matter of 'when'.*"[4]

Following that, national activities were undertaken in different countries to establish the

[1]*From the Department of Information Technology, University Medical Center of the Johannes Gutenberg University, Langenbeckstrasse 1, 55131 Mainz, Germany.*

[2]*From the Department of Internal Medicine II, University Medical Center of the Johannes Gutenberg University, Langenbeckstrasse 1, 55131 Mainz, Germany.*

Correspondence to: Johannes Peter Fritsch, Department of Information Technology, University Medical Center of the Johannes Gutenberg University, Langenbeckstrasse 1, 55131 Mainz, Germany; tel: +49-6131-17483832; fax: +49-6131-17473832; e-mail: jp.fritsch@unimedizin-mainz.de

Online publication 19 February 2010

doi: 10.1007/s10278-010-9275-8

adoption of irreversible image compression in clinical practice. In February 2008, working groups of the German Roentgen Society organized a consensus conference to define the maximum accepted compression as a recommendation for radiologists.[5] In April 2008, the Royal College of Radiologists in the United Kingdom published 'recommended levels of compression for different modalities for the purpose of primary diagnosis'.[6] At the same time, Canadian activities resulted in a similar recommendation.[7]

There is now general agreement on the use of compression for visual assessment of coronary obstructions, when applying irreversible JPEG compression in the range up to factors of 8:1 or 10:1.[8–17] Some detailed studies on quantitative coronary angiography (QCA), however, have resulted in much lower compression limits, while the results of other investigations on QCA pointed to an even higher compression tolerance.

The aim of this analysis is to resolve this disturbing discrepancy in thoroughly conducted QCA studies. The discrepancy between the high compression tolerance found in the studies on visual content and the low tolerance reported by some of the quantitative studies shall be explained at the same time.

Table 1 gives an overview of the results of the published studies on the effect of irreversible JPEG compression on QCA. These results can be divided into two groups. When considering the lower estimates, the compression ratio is limited to a small value (≤6:1). The authors of these studies agreed that QCA algorithms are very sensitive to artifacts that are induced by JPEG compression. On the other hand, there is the second group of studies that agrees on allowing large compression ratios (typically 12:1) with the conclusion that QCA algorithms are rather insensitive concerning irreversible JPEG compression.

Table 1. Maximum Compression Ratio (CR) for the use of JPEG in QCA

Publication	Max. CR
Whiting et al.[32]	≥20:1
Rigolin et al.[14]	≥15:1
Koning et al.[13]	<5:1
Slump et al.[33]	≥12:1
Tuinenburg et al.[16]	≤6:1

To resolve the discrepancy, this study analyzes the results of the evaluation of clinical coronary angiograms and of two kinds of phantom vessel images (physical and computer phantoms) for the first time in a common experimental design, instead of assessing them in separate studies. This allows the examination of the influence of X-ray quantum noise that the above-mentioned QCA studies did not take into consideration. The development of a modified QCA algorithm that offers a spatial resolution of 0.1 pixels was a prerequisite for this analysis. This algorithm is based on an edge detection procedure frequently used in previous scientific QCA studies.

MATERIALS AND METHODS

Images

Three sets of images were used: (1) coronary angiograms from clinical routine, (2) images of perspex phantom vessels, and (3) images of phantom vessels obtained by computer simulation. The coronary angiograms and the images of perspex phantoms were acquired at a digital catheterization laboratory (Siemens HICOR) at a standard X-ray exposure of 0.18 μGy per frame. The angiograms selected were acquired with an image intensifier input screen diameter of 12 cm. The perspex phantoms were acquired utilizing two image intensifier input screen diameter sizes: 17 cm, often used in coronary angiography and 12 cm, the minimum input screen diameter providing maximum enlargement and mainly used in interventional procedures.

The images have a spatial resolution of 512 × 512 pixels, resulting in a pixel size of 0.25 mm (12 cm input screen diameter) and 0.35 mm (17 cm input screen diameter). The gray value resolution is 8 bit.

Digital Coronary Angiograms

The coronary angiograms were routinely acquired at the cardiac catheterization laboratory of the University Hospital of Mainz, Germany, with a Siemens HICOR system, using X-ray contrast dye with the usual concentration of 370 mg/ml iodine. The angiograms from 48 patients, who underwent routine diagnostic or interventional procedures, were

chosen at random. One hundred thirty-one images, appropriate for QCA analysis, were selected from the cine runs of these patients. Each of these images was taken from a different sequence. On these images, 158 vessel segments were selected with a coronary stenosis.

Images of Perspex Phantom Vessels

Perspex tubes (Arri, Munich, Germany) with precision drillings (0.7 mm up to 5.5 mm) were used. They were filled with contrast dye Urografin (Schering, Berlin, Germany) using concentrations of 370 and 200 mg/ml iodine. The acquisition was carried out using water as a patient-equivalent scattering medium.

Simulated Phantom Vessel Images

Phantom vessel images were calculated for image intensifier input diameter values of 12 and 17 cm and contrast dye concentrations of 200 and 370 mg/ml iodine. The calculations used settings for quantum noise and aperture that are clinically relevant.[18] Images were calculated for vessel diameters between 3 and 25 pixels, in steps of 0.5 pixels. The QCA algorithm used allows do determine edges with a resolution of 0.1 pixels. For this reason, for each diameter value, vessel images were calculated with the vessel position shifted relative to the pixel raster in 0.1 pixel steps. This resulted in ten images for each diameter value.

Quantum Noise

Noise in medical X-ray images is mainly caused by the quantum structure of the X-ray beam. At the typical dose rate per frame of about 0.2 μGy applied in angiocardiography, the number of quanta is small enough to give rise to detectable statistical fluctuations, the quantum noise, which cause the well-known quantum mottle ("salt-and-pepper" noise) in the images. This mottle does not usually affect the visual analysis of the images. On the other hand, quantitative analyses, making use of local image information on a pixel basis, have to take quantum noise into account. In computerized edge detection, the smoothing of the underlying pixel data during edge detection and the smoothing of the resulting edges reduces the influence of quantum noise but reduces also the sensitivity of the edge detection. Therefore, only a moderate smoothing of data can be performed.

Image Compression

Image compression was achieved using the JPEG standard. The JPEG quality factor controls the quantity of compression in the JPEG algorithm. The resulting compression factor depends on the content of the images. In this study, JPEG quality factors between 100 and 70 were used. Figure 1 shows the relationship between the JPEG quality factor and the average compression factor for the coronary angiograms used.

Quantitative Coronary Angiography

QCA is an objective method to measure the geometrical dimensions of vessels. The use of computer-aided automatic edge detection results in more exact and reproducible results than visual estimates.[19,20] QCA is still based on two-dimensional X-ray images of the three-dimensional contrast-filled vessel lumen. Therefore, the current standard quantitative methods focus on the projection of the vessel. However, research on three-dimensional QCA[21,22] and on the integration of QCA with intracoronary ultrasound[23,24] is making progress.

The QCA technique used for this study is based on an automated edge detection algorithm, applied to single frames of angiographic scenes. These frames are displayed on the QCA workstation. Using the system mouse, the operator indicates, on the selected image, the beginning and end of the

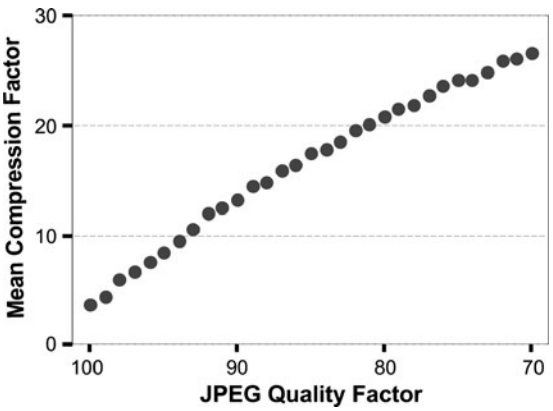

Fig 1. Relationship between compression factor and JPEG quality factor for coronary angiograms.

vessel segment to be analyzed. After this, a path line through the segment of interest is automatically computed. Alternatively, the user may indicate the approximate midline of the vessel segment. For successive lines perpendicular to this midline, the algorithm identifies the vessel edge points based on the values of the convolution of the brightness profiles with a predefined convolution kernel. A dynamic path search with a minimum cost algorithm finally supplies the vessel edges.[25]

In a second iteration, a new midline is automatically generated according to the position of the initial edges, and then the final edges are determined as before. The edges are smoothed using a least squares fit and are displayed on the screen. After the final edges have been detected, the diameter function is determined from the left- and right-hand edge positions, allowing the further assessment of relevant clinical parameters.

The software used in this study allows the storage and the later use of the midline data from the second iteration of edge detection described above, so that exactly the same midline can be used in the evaluation of the corresponding compressed images. Using the same midline in all measurements of the same vessel ensures that the vessel is always examined identically, i.e., at the same locations.

Convolution Kernels

Two kinds of convolution kernels, representing typical methods for edge detection,[26] were used. The size of the convolution kernel was 5 points. Figure 2 shows the convolution kernels for the left edge of the gray value profile of the vessel. The corresponding kernels for the right edge are obtained by mirroring the left edge kernel at the vertical axis.

The first derivative of the gray value profile and cubic smoothing with the method of least squares determine the edge position, using kernel 1.[27] Convolution with kernel 2 is equivalent to matching an edge profile with the gray value profile.[28] A modified high-resolution algorithm was used that enables the determination of the edge positions with a resolution of 0.1 pixels.[10]

Measurement Routine

The uncompressed images were analyzed interactively by an experienced user. The accompanying midline was stored together with the resulting edge data. This midline was uploaded and reused in the subsequent automated analyses of the corresponding compressed images.

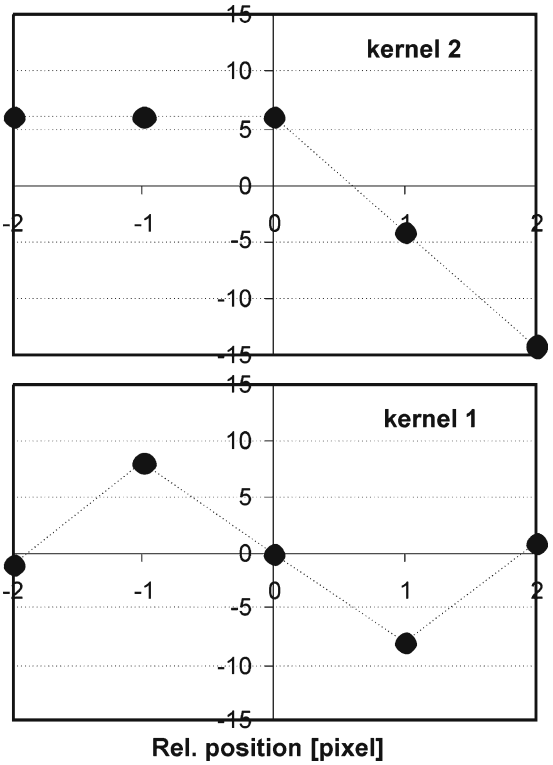

Fig 2. Convolution kernels used for edge detection (*left edge*).

Preliminary investigations indicated that the vessel/edge position relative to the 8×8-pixel-block boundaries of the JPEG algorithm affects the results of QCA in the compressed image. To take this into consideration, repeated measurements were performed with each image, shifting the image (and the corresponding midline) relative to the block boundaries. This shift was performed automatically by the computer, horizontally, parallel to the pixel raster, in steps of 1 pixel. Thus, eight positions resulted in eight evaluations for each image.

Measured Parameters

In the phantom images, the mean value and standard deviation of the diameter were determined along the homogeneous (i.e., with constant true diameter) vessel segments. In addition to this, the local diameter was examined, and its change due to compression was determined in order to

compare the results with those of the analysis of coronary angiograms. In the coronary angiograms, the minimum vessel diameter of the examined vessel section was selected as a special case of the local diameter, and the compression-induced change of the minimum vessel diameter was determined. No calibration was carried out. Only pixel values were examined.

For each of the underlying primary images, the results of the shifted images (see "Measurement Routine" section) were summarized to get the overall compression effect. For the same reason, the results of the images with shifted vessel positions (subpixel shifts) were summarized for each of the underlying true diameter values for the simulated phantom images.

RESULTS

Only the results for kernel 1 are presented here, since all relevant inferences from the results for kernel 1 are also valid for kernel 2. Furthermore, only the results of the 12 cm image intensifier images are presented because these images are the most sensitive to compression and therefore, affected the most. The results obtained from the 17 cm image intensifier images are more or less inversely proportional to the image intensifier diameter; in this case, the factor is 12/17. This behavior is analogous to the corresponding changes of the signal to noise ratio of quantum noise. The signal to noise ratio is proportional to the square root of the number of X-ray quanta, which is proportional to the pixel area. This area corresponds to the square of image intensifier diameter value.

Figure 3 shows the results of the analysis of the coronary images. The compression-induced change of the minimum diameter of a defined vessel segment was analyzed. The associated minimum diameter in the uncompressed image served as the reference value. For each of the JPEG quality factors examined and for all coronary angiograms, the changes were summarized by the mean value and standard deviation. These values are plotted as a function of the JPEG quality factor.

The results of the corresponding analysis of the images of the perspex phantom vessels are shown in Fig. 4. In this analysis, the change of local

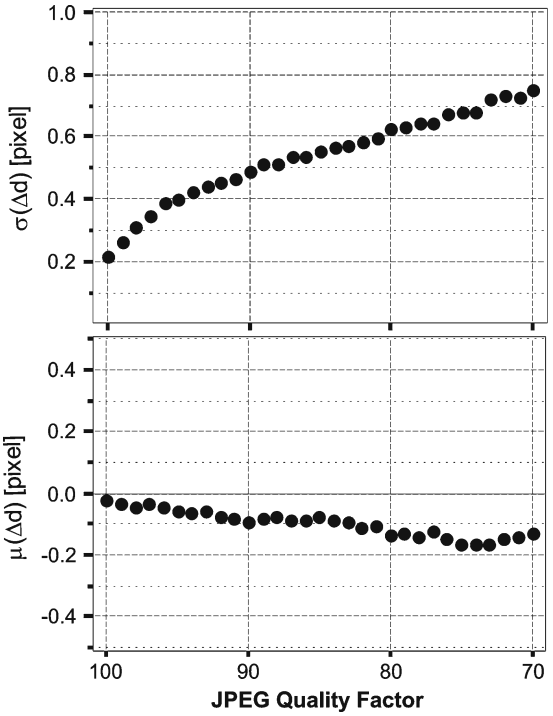

Fig 3. Compression-induced changes of the minimal luminal diameter of defined vessel segments of coronary angiograms.

diameter, due to compression, was determined. Again, for all the phantom images examined, at each of the JPEG quality factors, the changes were summarized by the mean value and standard deviation.

The results are comparable to those obtained from the analysis of the coronary angiograms. At the contrast dye concentration usually applied in coronary angiography, the standard deviation is a little smaller for the phantom vessel images than it is for the coronary angiograms. This can be explained by additional sources of error in clinical coronary angiography, e.g., inhomogeneous background of the analyzed vessel segments, differing quality of radiation, incomplete replacement of the blood by contrast dye, or varying mixture of the contrast dye with blood, corresponding to variations in contrast dye concentration.

Clearly smaller effects of compression can be observed when looking at the change of the total diameter of the vessel phantoms. In Fig. 5, the compression-induced changes of standard deviation ($\Delta\sigma$) and of mean value ($\Delta\mu$) of diameter are plotted as a function of the JPEG quality factor. The changes have been summarized for the diameter range examined, without differentiating

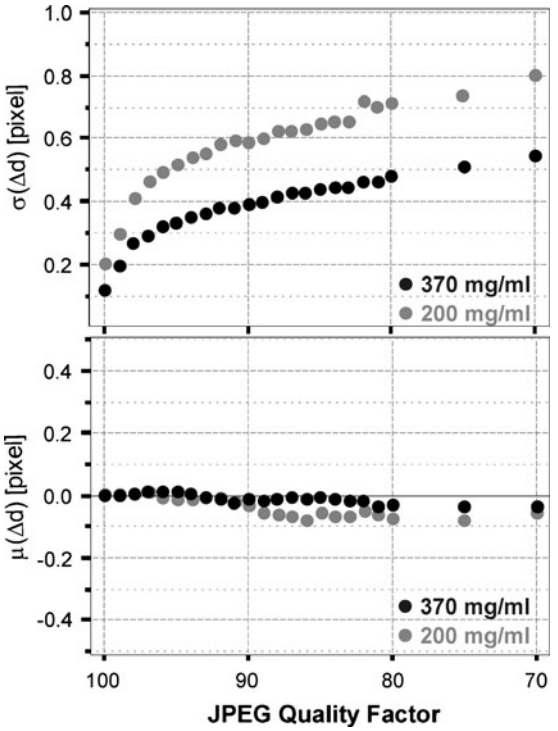

Fig 4. Compression-induced change of the local diameter of perspex phantom vessels.

between the phantom diameter values, since only the range of changes, i.e., the maximum change is of interest. The results are plotted as box and whisker plot; outliers and extreme cases are represented as diamond-shaped points.

To explain this difference in the effects of compression, the compression-induced changes have to be investigated in detail.

Assessing the Role of Quantum Noise

Considering a vessel with constant true diameter (i.e., a phantom), compression clearly has a larger influence on the local diameter value, determined by QCA, than on the mean value of the diameter. It is important to note that for the diameter mean value (which approximates to the true diameter value) the influence of quantum noise is strongly reduced. This is due to averaging, while in local diameter measurements this influence is present. When the results depend on the choice of mean diameter or local diameter as the reference, this is evidence for an interaction of quantum noise and compression.

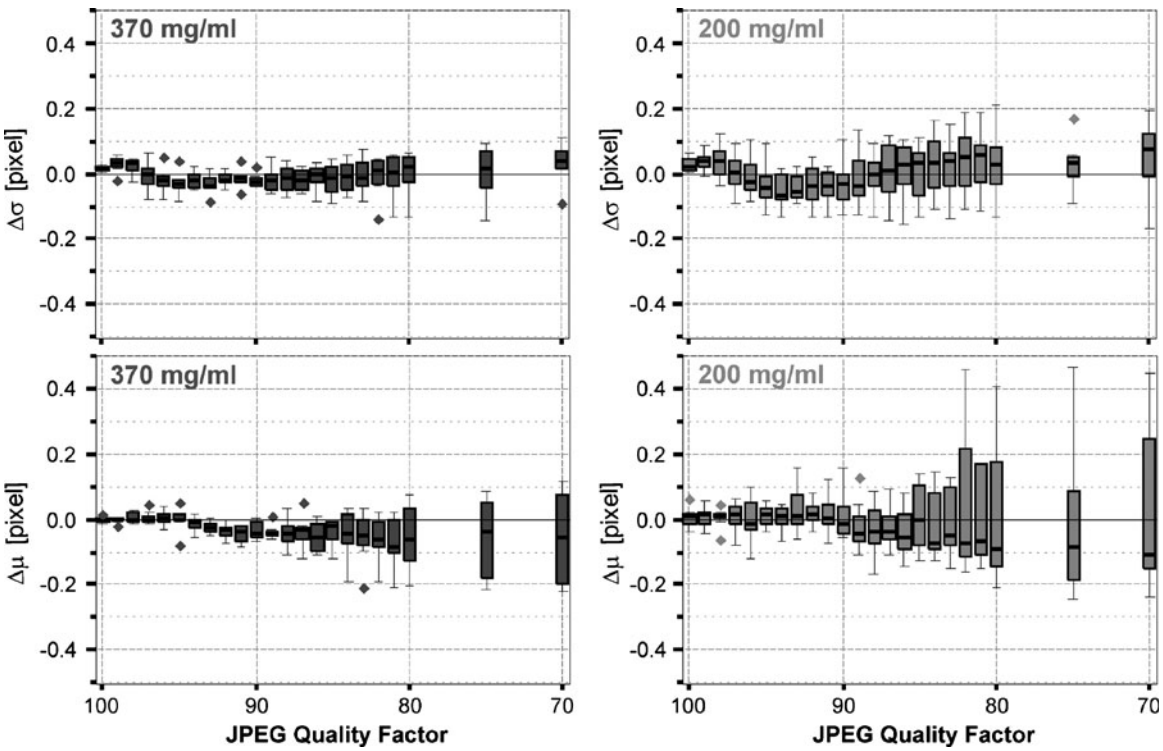

Fig 5. Compression-induced changes of the diameter of perspex phantom vessels.

This interaction can be examined in detail by a discussion of the results from the simulated phantom images. The exact magnitudes of the measured values mainly depend on the contrast dye concentration and the X-ray dose applied for the simulation. Thus, they may vary with the images examined. However, the basic findings are universally applicable. Experiments, using images of perspex phantom vessels, have confirmed these findings.

In this study, where simulated phantoms are used that provide constant diameters, there are two main sources of the variability in the diameters measured: the noisy structure superimposed on the ideal X-ray image by quantum effects and the variability induced by irreversible compression of the noisy images. In the uncompressed image, variability is caused by quantum noise. For that reason, even in the simulated angiographic images with their ideal geometry, different values of the diameter *d0* are measured at different locations along the artificial vessel. The mean value ($\mu 0$) of the corresponding distribution approximates the true diameter.

In Fig. 6, a special representation has been chosen to show the relationship of the diameter values *d0*, which are measured in the uncompressed original image, with those measured in the compressed image, *d*. For that, the diameter values have been measured at corresponding locations

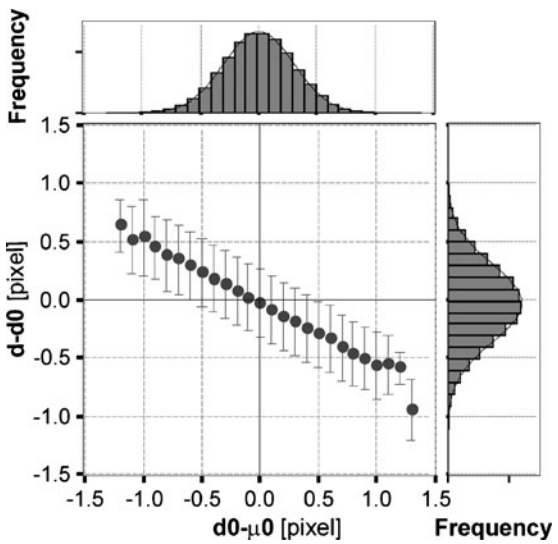

Fig 6. Distributions of the compression-induced changes of diameter value as a function of the change of diameter caused by quantum noise in the uncompressed image (simulated phantom images, JPEG quality factor 90).

along the vessel in the uncompressed image and the compressed image. The data have been acquired at JPEG quality factor 90, using simulated phantom images. The compression-induced change of diameter ($d-d0$) is plotted as a function of diameter change caused by quantum noise in the uncompressed image ($d0-\mu 0$). The discrete values for $d0-\mu 0$ are due to the spatial resolution of the QCA algorithm. The projection plotted along the vertical axis shows the corresponding distribution of diameter changes caused by compression, while the projection above the horizontal axis supplies the distribution of the changes of diameter due to quantum noise.

The simplest theory would predict that the two sources of variability (quantum noise and compression) should add up. As a result, the diameter values at those locations, which contribute to a particular value of *d0* in the uncompressed image, after compression would be distributed around this value, while their mean value would remain at the particular value of *d0*. To test this first-order prediction, the values of the two described diameter distributions are subtracted from the mean values of these distributions, obtaining the distributions of diameter changes:

- Change due to quantum noise: $\Delta_{\text{roentgen}} = d0-\mu 0$
- Change due to compression: $\Delta_{\text{compression}} = d-d0$

For the simple model of an additive effect of random compression noise, a vanishing mean value of $\boldsymbol{\Delta}_{\text{compression}}$ would be expected. In Fig. 6, the distributions of the associated compression-induced diameter changes ($\boldsymbol{\Delta}_{\text{compression}}$) are shown as a function of the change due to quantum noise ($\boldsymbol{\Delta}_{\text{roentgen}}$). The dots mark the mean values and the bars represent the standard deviations. Compression-induced variability is added to the existing variability, as expected. The measured values with original diameter *d0* (resp. diameter change $\boldsymbol{\Delta}_{\text{roentgen}}$) show an additional variability after compression (see error bars). This effect of compression is quite homogeneous for the different values of *d0* resp. $d0-\mu 0$.

Nevertheless, there is a deviation from the simplifying prediction that the mean values of the respective distributions should lie on the horizontal axis. In Fig. 6, a systematic change of these mean values is observed. The quantity of this change shows a *negative* correlation with $\boldsymbol{\Delta}_{\text{roentgen}}$. Those diameter values, which were underestimated

before compression, become larger after compression, while larger ones become smaller. Thus, the measurement variability due to quantum noise is effectively reduced. This is in accordance with the theoretical prediction and the visual observation, indicating that the JPEG compression procedure works like a low-pass filter in the spatial frequency domain and therefore, reduces the high frequency component of quantum noise.[3,10,29]

A more systematic analysis is possible by dividing the compression-induced changes of the diameter into the contributions that are due to the different initial diameter values, *d0*, in the uncompressed image. This can be done mathematically (see Appendix). Figure 7 shows the results of the division for an image of a perspex phantom vessel with a typical vessel diameter of 3 mm. With the compression procedure used, the contribution of the high frequency quantum noise ($\sigma_{roentgen}$) is reduced. Simultaneously, a compression-induced noise ($\sigma_{compression}$) appears. In the measurements, this effect appeared in the range of JPEG quality factor between 100 and 95. Below quality factor 90, the contribution of the quantum noise to the total noise drops to a small part. The total noise then mainly consists of the contribution of compression. These considerations make the small net effect of the compression for the total variability (σ_{total}) plausible.

DISCUSSION

If the original image is used as the reference, this results in a bias against compression, because any difference can only favor uncompressed images.[3] The isolated view at the compression-induced changes of the local diameter leads to incorrect interpretations, when discussing the influence of compression on the results of QCA. This discussion must take into account the fact that the reference, which is the measured local diameter value in the uncompressed image, is generally different from the true value that is measured in an image without presence of quantum noise. The deviation of the measured value from the true diameter is essential for the determination of the influence of compression. However, this true diameter cannot be locally determined, since local diameter values imply deviations induced by quantum noise.

This has been demonstrated by the evaluation of the phantom images. If the changes refer to the mean value of the phantom vessel diameter, this results in clearly smaller compression effects than if the changes refer to the local diameter (cp. Figs. 4 and 5). This is due to the described interaction of quantum noise and compression. The decrease, due to compression, of the influence of quantum noise gives rise to changes of the local diameter. These changes must not to be interpreted as degradation in the sense of a distortion of the measured values, since statistically the measured local diameter moves closer to the true diameter value. Observing only the local diameter, any compression-induced change is interpreted as degradation.

When using coronary vessels, the true local diameter value is not known. Nevertheless, the true

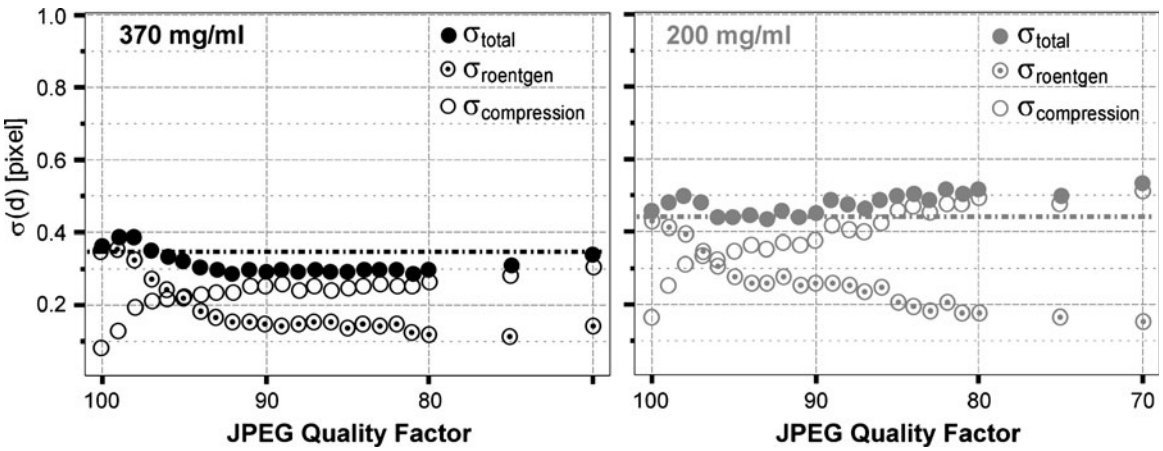

Fig 7. Division of the total standard deviation of diameter into the part due to quantum noise and the compression-induced part, for a perspex vessel image (vessel diameter = 3 mm).

impact of compression on the patient images can be deduced from the results of the phantom images: In the phantom images, additionally analyzed in the study, it is possible to determine the true diameter value, using the mean value of the diameter values along the phantom vessel. The reference to this mean value, for the calculation of systematical and random effects of compression, results in the assessment of the true impact of compression for the phantom vessels. The accompanying analysis of the local diameter of the phantom vessels makes it possible to relate the results of the evaluation of the phantom images to those of the patient images. In this way, the true impact of compression for the patient images can be concluded from the results of the phantom images. To do this, the same imaging conditions as for the coronary angiographic images have to be applied when simulating phantom images.

In summary, the mean diameter measured in a homogeneous vessel segment (i.e., a segment with constant true diameter) has to provide the reference for all variability measurements in compression studies. Since such homogeneous vessel segments can be found only approximately within coronary angiograms (except for the catheter), the use of homogeneous phantom vessel images is preferable in basic studies of image data compression. It could be argued that this type of phantom studies cannot exclude a loss in the relevant fine structure of lesions due to compression. The two independent international studies on visual image quality mentioned above,[9,11] however, have indicated that no such critical loss of lesion structure accompanies the low-pass effect of the compression algorithm. In one of these studies,[9] even a compression-induced *enhancement* of visual lesion imaging quality was reported by several observers at low compression factors, an effect assessed even more quantitatively by this study.

Resolving the Discrepancies of the Previously Published Data

The results prompt a more detailed look at the studies for validity of image compression, specified in Table 1. The additional information specified in Table 2 shows the variations in the methods applied. In some cases, the mean diameter was measured, in others, the minimum local diameter. Most of the studies applied QCA to coronary angiograms, only in one case to simulated phantom vessels. It is easily recognized that in the group of studies, which resulted in a limited range of permissible compression (≤6:1), the local diameter of coronary vessels was analyzed. As shown above, this mode of evaluation results in a compression limit, which is unrealistically low. The discrepancies between the maximal compression ratios can be explained and resolved with the results of this study.

Table 2. Maximum Compression Ratio (CR) for the use of JPEG in QCA

Publication	Max. CR	Measured Parameter/Object	
Whiting et al.[32]	≥20:1	Mean diameter	Simulated phantom vessels
Rigolin et al.[14]	≥15:1	Mean diameter	Coronary vessel segments
Koning et al.[13]	<5:1	Local diameter	Coronary vessel segments
Slump et al.[33]	≥12:1	Mean diameter	Coronary vessel segments
Tuinenburg et al.[16]	≤6:1	Local diameter	Coronary vessel segments

Influence of the Compression-induced Changes of the Diameter on the Overall Result

The analysis of the compression-induced change of the diameter of phantom vessels shows only small effects at the contrast dye concentration 370 mg/ml, usually applied in coronary angiography. The changes of mean value and standard deviation of diameter are lower than 0.1 pixels up to the limit of compression, given by the aesthetic image quality at JPEG quality factor 93 (compression factor of 10[10]). Over the entire range of compression examined, the changes are lower than 0.2 pixels.

To evaluate the relevance of this change, the different contributions to the variability of the measured diameter have to be taken into consideration. In addition to the quantum noise already considered, variations due to the patient, the angiographic procedure, and frame selection for image analysis contribute to variability. The literature reports a total value of 0.14–0.17 mm for these contributions to total QCA error.[30,31] This corresponds to about 0.6–0.7 pixels at the

used image intensifier input diameter of 12 cm. These additional errors are statistically independent contributions, so that their square values have to be added to the variance measured without these contributions. A standard deviation, due to quantum noise, of 0.4 pixels (determined from phantom images) is assumed. With that, a compression-induced additional noise of 0.2 pixels results in an increase in the total variability of the measured diameter of less than 0.1 pixels, corresponding to 0.025 mm. This increase is irrelevant and can be neglected. The systematic compression-induced change of diameter, which is smaller than 0.025 mm within the analyzed range of JPEG quality factor, can also be neglected.

CONCLUSION

JPEG compression interacts with the quantum noise of X-ray images. At limited compression factors, the JPEG compression/decompression procedure is equivalent to a low-pass filter in the spatial frequency domain and therefore, reduces the high frequency component of quantum noise. For this reason, the impact of the compression on the results of quantitative coronary angiography has been overestimated in some literature, by interpreting any change in local diameter as an error due to compression, while disregarding the beneficial effect of compression on quantum noise. So in previous studies the results from the uncompressed images should not have been used as reference, since they are biased as well. By taking into consideration the quantitative effect of quantum noise in QCA, the influence of JPEG compression can be neglected for compression factors up to ten at clinically applicable X-ray doses. This limit is comparable to that found by visual analysis for aesthetic image quality. The design of future studies on image compression effects, applying advanced imaging or measurement techniques, should take the interaction with quantum noise explicitly into consideration.

APPENDIX

For a vessel with constant true diameter (phantom), the total standard deviation σ of the measured diameter along the vessel in the compressed image

$$\sigma_{total}^2 = \frac{1}{N} \cdot \sum_{l=1}^{N} (d(l) - \mu)^2, \mu = \frac{1}{N} \cdot \sum_{l=1}^{N} d(l)$$

$l = 1 \ldots N$ location along the vessel where the vessel diameter is measured

$d(l)$ local diameter at location l measured in compressed image

can be transformed as follows, grouping the diameter values by the corresponding values in the uncompressed image instead of by location:

$$\sigma_{total}^2 = \tfrac{1}{N} \cdot \sum_{l=1}^{N} d^2(l) - \mu^2 = \tfrac{1}{N} \cdot \left(\left(\sum_{l}^{N_1} d_1^2(l) + \sum_{l}^{N_2} d_2^2(l) + \ldots + \sum_{l}^{N_n} d_n^2(l) \right) \right) - \mu^2$$

$$= \tfrac{1}{N} \cdot \left(\left(\sum_{j}^{N_1} d_{1j}^2 + \sum_{j}^{N_2} d_{2j}^2 + \ldots + \sum_{j}^{N_n} d_{nj}^2 \right) \right) - \mu^2$$

$d_i(l)$ local diameter at location l with corresponding diameter value $d0_i$ in the uncompressed image; the diameter $d0_i$ describes the influence of quantum noise

d_{ij} local diameter with corresponding diameter value $d0_i$ in uncompressed image with index j differentiating the different values

N_i frequency of occurrence of $d0_i$; $N_1 + N_2 + \ldots + N_n = N$

Using the relationship

$$\frac{1}{N_i} \cdot \sum_{j}^{N_i} d_{ij}^2 = \sigma_i^2 + \mu_i^2$$

σ_i standard deviation of the N_i diameter values with initial diameter $d0_i$ around the mean value μ_i

it results in

$$\sigma^2_{total} = \frac{1}{N}\cdot\left(N_1\cdot\left(\sigma_1^2+\mu_1^2\right)+N_2\cdot\left(\sigma_2^2+\mu_2^2\right)+\ldots+N_n\cdot\left(\sigma_n^2+\mu_n^2\right)\right)-\mu^2$$
$$= \underbrace{\frac{1}{N}\cdot\left(N_1\cdot\sigma_1^2+N_2\cdot\sigma_2^2+\ldots+N_n\cdot\sigma_n^2\right)}_{\sigma^2_{compression}} + \underbrace{\frac{1}{N}\cdot\left(N_1\cdot\mu_1^2+N_2\cdot\mu_2^2+\ldots+N_n\cdot\mu_n^2\right)-\mu^2}_{\sigma^2_{roentgen}}$$

Thus, the total standard deviation of diameter is divided into compression dependent $\sigma_{compression}$ and $\sigma_{roentgen}$ that comes from the distribution of diameter values in the uncompressed image. Without compression, the equation above describes the standard deviation of diameter *d0* due to quantum noise. In this case, μ_i corresponds to $d0_i$, and σ_i results in zero.

REFERENCES

1. ISO/IEC 10918 (JPEG) Digital compression and coding of continuous-tone still images.
2. Seeram E: Irreversible Compression in digital radiology. A literature review. Radiography 12:45–59, 2006
3. Erickson BJ: Irreversible Compression on Medical Images. Society for Computer Applications in Radiology, White Paper, 2000. Available at http://www.scarnet.org/WorkArea/showcontent.aspx?id=1208. Accessed 25 May 2009
4. Bak PRG: Will the use of Irreversible Compression become a standard of practice? SCAR News 18(1):10, 2006
5. Loose R, Braunschweig R, Kotter E, Mildenberger P, Simmler R, Wucherer M: Compression of Digital Images in Radiology—Results of a Consensus Conference. Fortschr Röntgenstr 181:32–37, 2009
6. The Royal College of Radiologists: The adoption of lossy image data compression for the purpose of clinical interpretation. London: The Royal College of Radiologists, 2008. Available at http://www.rcr.ac.uk/docs/radiology/pdf/IT_guidance_ LossyApr08.pdf. Accessed 25 May 2009
7. Koff D, Bak P, Brownriff P, Hosseinzadeh D, Khademi A, Kiss A, Lepanto L, Michalak T, Shulman H, Volkening A: Pan-Canadian Evaluation of Irreversible Compression Ratios („Lossy Compression“) for Development of National Guidelines. J Digit Imaging, doi:10.1007/s10278-008-9139-7, October 18, 2008
8. Baker WA, Hearne SE, Spero LA, Morris KG, Harrington RA, Sketch MH, Behar VS, Kong Y, Peter RH, Bashore TM, Harrison JK, Cusma JT: Lossy (15:1) JPEG compression of digital coronary angiograms does not limit detection of subtle morphological features. Circulation 96:1157–1164, 1997
9. Brennecke R, Bürgel U, Simon R, Rippin G, Fritsch HP, Becker T, Nissen SE: American College of Cardiology/European Society of Cardiology international study of angiographic data compression phase III: Measurement of image quality differences at varying levels of data compression. Eur Heart J 21:687–696, 2000
10. Fritsch JP: Computergestützte und psychovisuelle Maße zur intersubjektiven Bewertung der Bildqualität von quellenkodierten Koronarangiogrammen [dissertation]. Johannes Gutenberg-Universität, Mainz, 2003
11. Kerensky RA, Cusma JT, Kubilis P, Simon R, Bashore TM, Hirshfeld JW, Holmes DR, Pepine CJ, Nissen SE: American College of Cardiology/European Society of Cardiology international study of angiographic data compression phase I: The effects of lossy data compression on recognition of diagnostic features in digital coronary angiography. Eur Heart J 21:668–678, 2000
12. Kirkeeide R, Beretta P, Smalling RW, Anderson HV, Schroth G, Gould KL: Diagnostic content of digital coronary arteriograms is unaffected by 12:1 image compression. J Am Coll Cardiol 29(Abstr Suppl):35A, 1997
13. Koning G, Beretta P, Zwart P, Hekking E, Reiber JHC: Effect of lossy data compression on quantitative coronary measurements. Int J Card Imaging 13:261–270, 1997
14. Rigolin VH, Robiolio PA, Spero LA, Harrawood BP, Morris KG, Fortin DF, Baker WA, Bashore TM, Cusma JT: Compression of digital coronary angiograms does not affect visual or quantitative assessment of coronary artery stenosis severity. Am J Cardiol 78:131–135, 1996
15. Silber S, Dörr R, Zindler G, Muhling H, Diebel T: Impact of various compression rates on interpretation of digital coronary angiograms. Int J Cardiol 60:195–200, 1997
16. Tuinenburg JC, Koning G, Hekking E, Zwindermann AH, Becker T, Simon R, Reiber JHC: American College of Cardiology/European Society of Cardiology international study of angiographic data compression phase II: The effects of varying JPEG data compression levels on the quantitative assessment of the degree of stenosis in digital coronary angiography. Eur Heart J 21:679–686, 2000
17. Whiting J, Eckstein M, Honig D, Gu S, Einav S, Eigler N: Effect of lossy image compression on observer performance in dynamically displayed digital coronary angiograms. Circulation 86 (suppl 1):I–444, 1992
18. Krass S: Beurteilung von krankhaften Veränderungen der Koronararterien auf Grund von Röntgenkontrastverfahren und intrakoronarem Ultraschallverfahren: Ein Methodenvergleich aufgrund quantitativer Kenngrößen [dissertation]. Johannes Gutenberg-Universität, Mainz, 1998

19. Garrone P, Biondi-Zoccai G, Salvetti I, Sina N, Sheiban I, Stella PR, Agostoni P: Quantitative Coronary Angiography in the Current Era: Principles and Applications. J Interv Cardiol, doi:10.1111/j.1540-8183.2009.00491.x, July 13, 2009

20. Fleming R, Kirkeeide RL, Smalling R, Gould KL: Patterns in visual interpretation of coronary arteriograms as detected by quantitative coronary arteriography. J Am Coll Cardiol 18:945–951, 1991

21. Gradaus R, Mathies K, Breithardt G, Böcker D: Clinical assessment of a new real time 3D quantitative coronary angiography system: Evaluation in stented vessel segments. Catheter Cardiovasc Interv 68:44–49, 2006

22. Agostoni P, Biondi-Zoccai G, Van Langenhove G, Cornelis K, Vermeersch P, Convens C, Vassanelli C, Van Den Heuvel P, Van Den Branden F, Verheye S: Comparison of assessment of native coronary arteries by standard versus three-dimensional coronary angiography. Am J Cardiol 102:272–279, 2008

23. Bourantas CV, Kalatzis FG, Papafaklis MI, Fotiadis DI, Tweddel AC, Kourtis IC, Katsouras CS, Michalis LK: ANGIO-CARE: An automated system for fast three-dimensional coronary reconstruction by integrating angiographic and intracoronary ultrasound data. Catheter Cardiovasc Interv 72:166–175, 2008

24. Sievers B, Böse D, Sack S, Philipp S, Wieneke H, Erbel R: Online PC-based integration of digital intracoronary ultrasound images into angiographic images during cardiac catheterization. Int J Cardiol 128:289–293, 2008

25. Pope DL, Parker DL, Clayton PD, Gustafson DE: Left ventricular border recognition using a dynamic search algorithm. Radiology 155:513–518, 1985

26. Reiber JHC: An overview of coronary quantitation techniques as of 1989. In: Reiber JHC, Serruys PW Eds. Quantitative coronary arteriography. Kluwer, Dordrecht, 1991, pp 55–132

27. Savitzky A, Golay MJ: Smoothing and differentiation of data by simplified least squares procedures. Anal Chem 36:1627–1639, 1964

28. Rosenfeld A, Kak AC: Digital picture processing. Academic, New York, 1976

29. Persons K, Palisson P, Manduca A, Erickson PJ, Savcenko V: An analytical look at the effects of compression on medical images. J Digit Imaging 10(suppl 1):60–66, 1997

30. Herrington DM, Siebes M, Sokol DK, Siu CO, Walford GD: Variability in measures of coronary lumen dimensions using quantitative coronary angiography. J Am Coll Cardiol 22:1068–1074, 1993

31. Reiber JHC, Koning G, von Land CD, van der Zwet PMJ: Why and how should QCA systems be validated? In: Reiber JHC, Serruys PW Eds. Progress in quantitative coronary angiography. Kluwer, Dordrecht, 1994, pp 33–48

32. Whiting J, Eckstein M, Morioka C, Staffel B, Eigler N: Lossy image compression has insignificant effect on the accuracy and precision of quantitative coronary angiography [abstract]. Circulation 88(suppl 1):I–652, 1993

33. Slump CH, Hagendoorn P, Rutgers R, de Bruijn FJ, Storm CJ, van Benthem AC: On the assessment of image compression quality by means of quantitative coronary angiography. SPIE proceedings 3031:708–719, 1997